ROOM -VENT '90

A2

Experimental study and numericalsimulation of natural convection in a room with heated ceiling or floor

F. Allard
C. Inard
J.P. Simoneau
Centre de Thermique INSA/CNRS
Villeurbanne Cedex, France

EXPERIMENTAL STUDY AND NUMERICAL SIMULATION OF NATURAL CONVECTION IN A ROOM WITH HEATED CEILING OR FLOOR.

F. ALLARD, C. INARD, J. P. SIMONEAU
Centre de Thermique INSA/CNRS
Bât 307 INSA F-69621 Villeurbanne Cedex

SUMMARY

This paper presents a study developed in the frame of the French national program about natural convection in buildings "A.R.C. Convection Naturelle dans l'Habitat". We focus here on the interaction between heated ceilings or floors and colder vertical walls. At first we describe our full scale experimental set up, built in a controlled thermal environment, and which enables us to reproduce most of the basic thermal boundary conditions found in a room in its natural climatic environment. Varying the external climatic condition of a vertical wall and the power injected in the horizontal walls, we characterize the global behavior of the room by its thermal field. Then, we present a numerical study of this problem in three steps. At first we show how numerical simulation at lower Rayleigh numbers can help us to a better understanding of natural convection even if they cannot pretend to represent the real problem. In a second step we used a Tchebycheff spectral method to study the unsteady regimes found at higher Rayleigh numbers, and pseudo-periodic solutions are found. The third step of this numerical experiment presents a k-ϵ model we developed, and it shows a good agreement between numerical results and experiments.

EXPERIMENTAL STUDY AND NUMERICAL SIMULATION OF NATURAL CONVECTION IN A ROOM WITH HEATED CEILING OR FLOOR.

F. ALLARD, C. INARD, J. P. SIMONEAU
Centre de Thermique INSA/CNRS
Bât 307 INSA F-69621 Villeurbanne Cedex

Introduction

Natural convection inside rooms is one of the main transfer phenomena by which the thermal power of a source is transferred to the inside air. Usually the thermal behavior and airflow patterns result from the activity of these sources and from the coupling of differentially heated walls.
In the case of heating systems using directly horizontal walls as heat sources, the coupling effect is even stronger. These systems have been used for a very long time, but the study of their convective behavior remains a difficult task. A carefull experimental analysis requires a well controlled environment, and direct numerical approach is still needing more research efforts.
In this study, we focus on the interaction between heated ceilings or floors and colder vertical walls. At first we describe our full scale experimental set up and present a set of results obtained by means of varying the outdoor climatic conditions and the power injected in the horizontal walls.
In a second part we develop a numerical analysis of natural convection in these two configurations using different levels of models. We start the numerical analysis with laminar solutions which lead us to a better understanding of the large stuctures of the flow patterns. Then, the introduction of a Tchebycheff Spectral model shows periodic behaviors of unsteady regimes found at higher Rayleigh numbers. Finally, the introduction of a two equation model of turbulence enables us to simulate real scale configurations.

Experimental Studies

MINIBAT Test cell

Figure 1 presents a longitudinal view of our experimental set up called MINIBAT (1,2). The main part of this experimental set up is a real scale room (3.1m x 3.1 m x 2.5m) built in a thermally controlled environment. Five of its walls are thermally guarded, the sixth one, the facade, is a 10mm thick glazing submitted on its external side to artificial outdoor climatic conditions generated by a climate simulator. This device is made of a thermal housing where the air temperature varies from -10°C to 30°C, and of a solar simulator built

of 12x1100W CSI lamps. This simulator provides solar lightings compatible with those found in a natural environment.
The ceiling is made of a 2.5cm thick plywood coated by a 5.5cm thick mineral wool. The internal surface of the ceiling received the same gypsum board layer as for the vertical walls of the cell. A resistive electrical film has been placed between the plywood and the gypsum-board to realize a uniform heating of the ceiling.

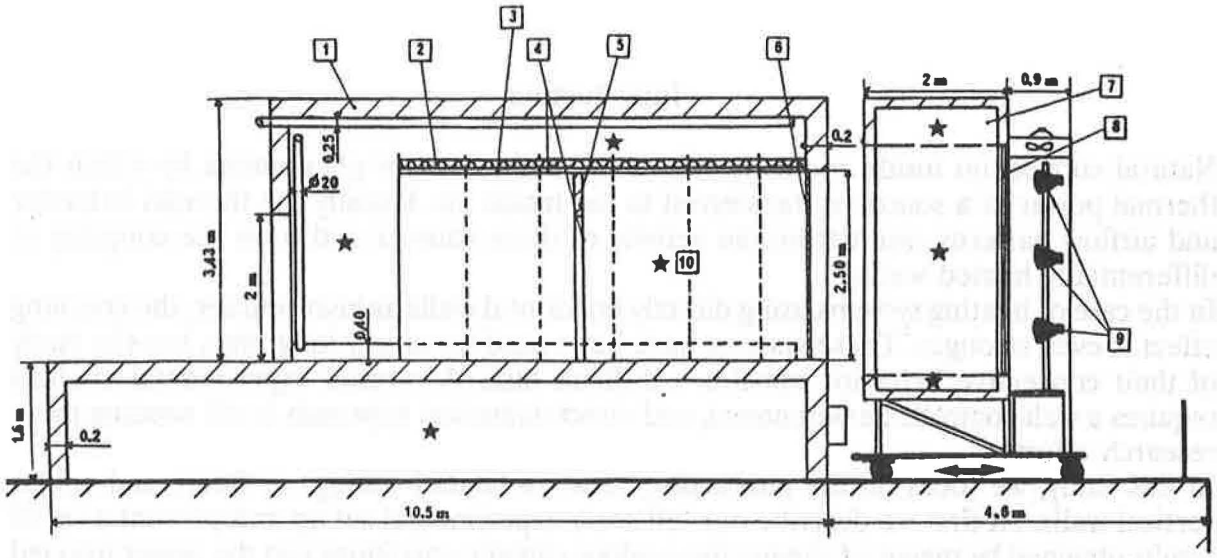

Fig. 1. Longitudinal Section of MINIBAT. (1) External envelop (cellular concrete e=.2m), (2) Fibreglass (e=.05m), (3) Plywood (e=.025m), (4) Gypsum-board (e=.01m), (5) Fibreboard (e=.05m), (6) Glazing (e=.01m), (7) Mobile Climatic Housing, (8) Double Glazing, (9) Solar Simulator, (10) Test Cell.

All the thermal and radiative properties of the materials used have been measured in our laboratory. In order to get the complete thermal field along the surfaces and inside the volume of the cell, 220 sensors are used. Most of them are devoted to air or surface temperature measurements. All these sensors have been calibrated in our laboratory, they are connected to a data acquisition system controlled by a PC which assumes the acquisition and a first local treatment of the data.

Studied configurations.

The configurations we consider in this paper are related to boundary conditions found inside a room of an intermediary level of a current building surrounded by other rooms at the same temperature. The only selected inputs are outdoor temperature, shortwave

lightings arriving inside the room and uniform heating of the ceiling.
In fact the behavior of the cell will result from the relative activity of two active surfaces:

* A horizontal wall (ceiling or floor)
* A vertical wall (facade)

In order to classify our experiments, we defined a reference temperature difference, a reference temperature and a reference Rayleigh number. The reference temperature T_0 is defined as the mean value of the average temperature of the colder and warmer walls.

$$T_0 = \frac{T_H + T_C}{2}$$

The reference temperature difference is the temperature difference beween these two walls.

$$\Delta T = T_H - T_C$$

All the temperatures are standardised using these two references, their dimensionless values vary finally from -0.5 to 0.5. The resulting Rayleigh number is calculated using the height of the cavity as reference for length, the reference temperature difference as temperature difference, and the reference temperature to calculate the air physical properties.

Heated Ceiling

Main Characteristics of the Experiments. In order to study the relative influence of the two active walls, we first vary the outdoor air temperature with a constant power injected in the ceiling, then we fix the oudoor conditions and we vary the injected power. Table 1 and 2 summarize the main characteristics of the experiments. We also mentionned in table 1 and 2 the variable r_c^* which represents the standardized vertical thermal gradient at the center of the room. This value results from a linear regression of the temperatures measured in five different altitudes (0.4, 0.75, 1.25, 1.75 and 2.10 m high). The Rayleigh numbers are beween 2.10^{10} and 6.10^{10}.

Thermal Stratification inside the Cavity. Figure 2 presents a typical result obtained for this first configuration. The isotherms presented here correspond to an outdoor air temperature of 0°C, and an injected power density of 97W/m². Figure 2 shows a typical example of thermal behavior of the cavity submitted to the coupled effects of a heated ceiling and a cold facade. This global behavior can be described in a first approach by the division of the room in three zones, a first strongly stratified zone just beneath the ceiling, an active cold boundary layer along the facade, and a regularly stratified core.

Variation of the outdoor air temperature. Varying the outdoor air temperature from -10°C to 20°C, and fixing the injected power density at the same level (97 W/m²), we always obtain a very similar behavior of the air contained in the cavity.

Table 1. Main Characteristics of the Experiments Realised with a Heating Ceiling System (Variation of outdoor temperature).

EXPERIM.	HC.1	HC.3	HC.4	HC.5	HC.6	HC.7
T_0 (°C)	22.57	27.57	30.16	32.78	34.95	37.73
ΔT (°C)	36.09	32.29	30.66	28.78	26.79	24.73
$Ra.10^{-9}$	56.9	47.1	42.9	38.7	34.8	30.8
T_c (°C)	17.86	22.03	24.34	26.55	28.24	30.76
T_c^*	-0.13	-0.17	-0.19	-0.22	-0.25	-0.28
r_c^*	0.21	0.19	0.18	0.18	0.17	0.19
$P(W/m^2)$	97.0	97.0	97.0	97.0	97.0	97.0

Table 2. Main Characteristics of the Experiments Realised with a Heating Ceiling System (Variation of injected power density).

EXPERIM.	HC.2	HC.8	HC.9	HC.10	HC.11
T_0 (°C)	24.73	19.38	14.44	10.48	7.88
ΔT (°C)	34.66	27.17	19.92	15.19	10.57
$Ra.10^{-9}$	52.8	45.1	35.8	29.2	21.2
T_c (°C)	19.30	16.84	14.03	11.84	10.50
T_c^*	-0.16	-0.09	-0.02	0.09	0.25
r_c^*	0.19	0.13	0.27	0.31	0.39
$P(W/m^2)$	97.0	63.0	38.0	17.0	14.0

To summarize we can say here that a variation of the outdoor air temperature leads to a translation of a dimensionless thermal profile, the deformations of this profile seem to be very small. This fact is illustrated by Fig. 3 , where the vertical temperature profile is drawn along the central vertical axis of the cavity.

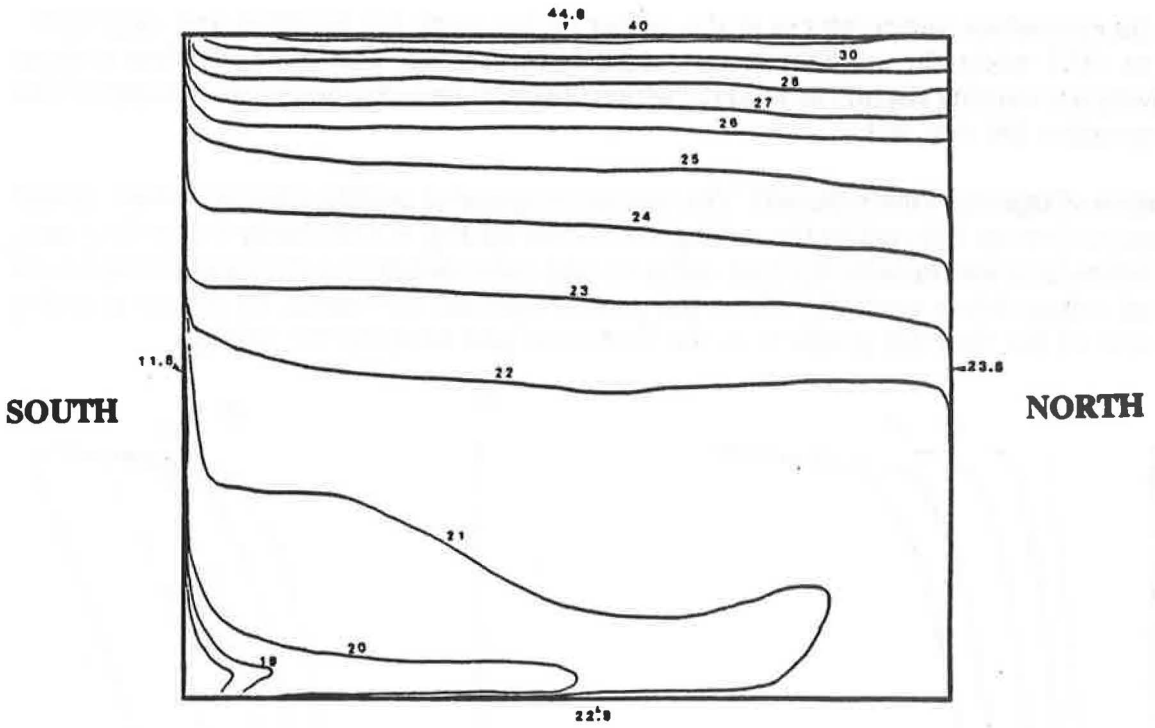

Fig. 2. Isothermal lines in the vertical mid plane of the cavity.

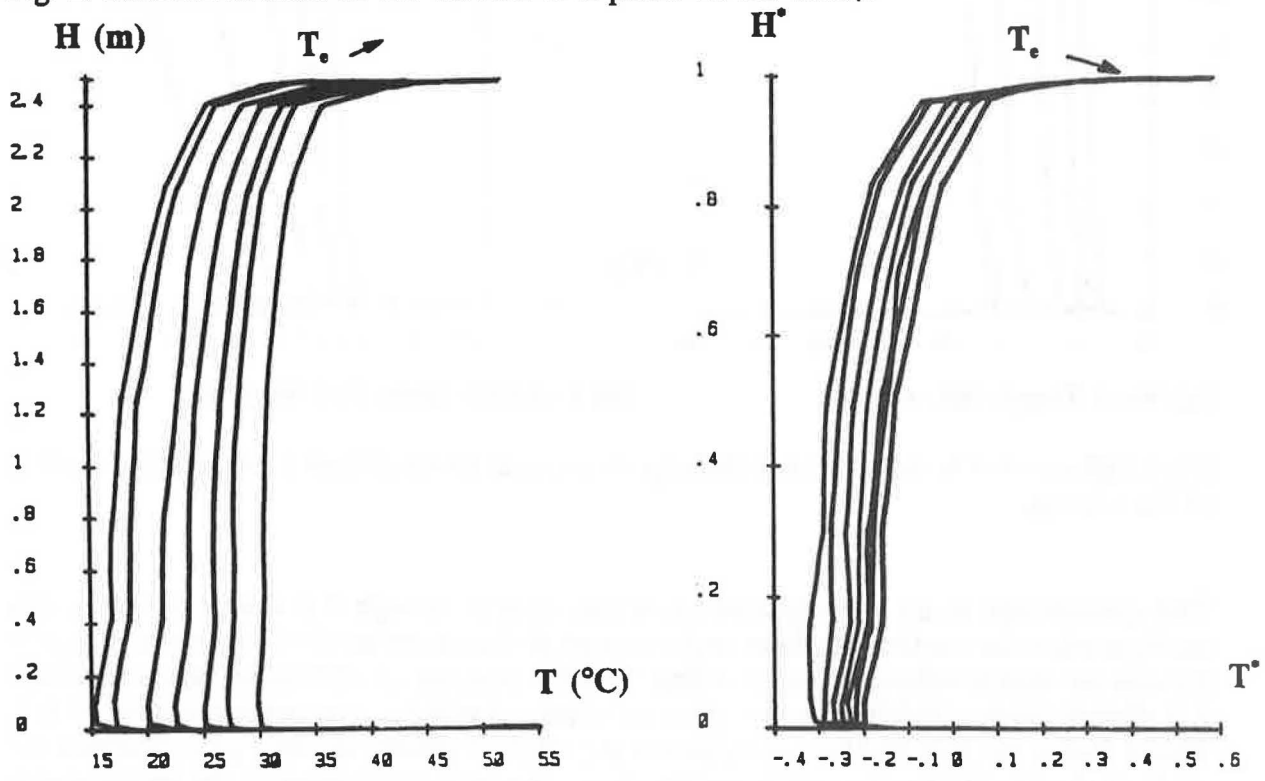

(a) Real Temperature (b) Dimensionless Temperature

Fig 3. Influence of Outdoor Air Temperature on Vertical Temperature Profiles at the Center of the Cavity.

The dimensionless temperatures at the center of the room are negative and vary from -0.28 to -0.13 when the outdoor temperature is increasing. The dimensionless vertical gradients are varying slightly around 0.2 which seems to be a characteristic number of this configuration for our cell.

Variation of Injected Power Density. The vertical temperatue profiles obtained when varying the power density injected in the ceiling are shown on Fig. 4. Contrarily to the first case, a variation in power density injected in the ceiling corresponds to a strong deformation of vertical temperature profiles. When the power injected decreases, we notice a strong decrease of the thermal gradient in the first zone just beneath the ceiling.

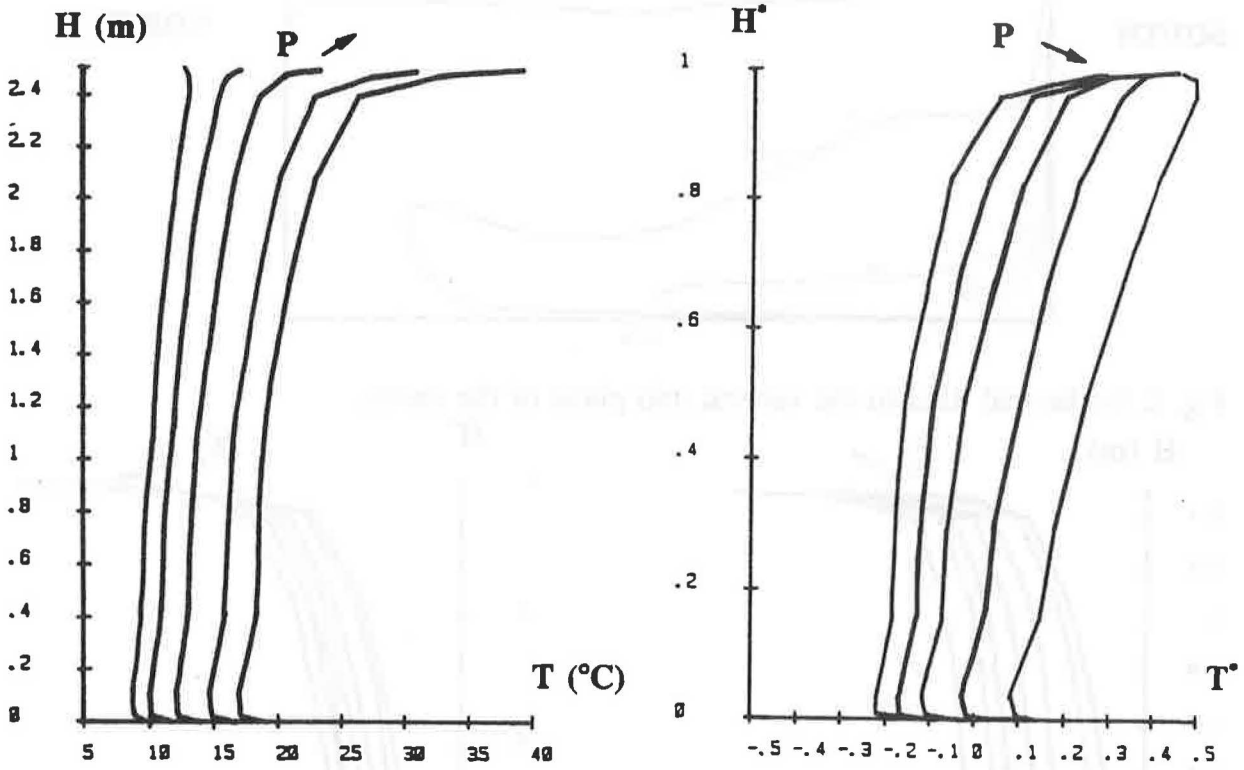

(a) Real Temperature (b) Dimensionless Temperature

Fig 4. Influence of Injected Power Density on Vertical Temperature Profiles at the Center of the Cavity.

This contributes to an homogenization of the profile through the whole cavity. In this configuration the vertical gradient at the center of the cavity tends of course to merge to the one we obtain without a heated ceiling. Nevertheless, for small injected power densities, it is slightly higher (0.40) than the value we obtained without any heating system (0.35) . This is due to the fact that for low values of the injected power, the flow pattern inside the cavity is dominated by the cold boundary layer, the global behavior of the cavity is very close to that of a non heated cavity. However, the upper part of the cavity is slightly overheated which explain higher value of the thermal gradient.

Heated floor

Main Characteristics of the Experiments. This configuration corresponds to a uniform solar lighting of the floor coupled with a vertical cold wall. It is a typical configuration of winter time in temperated regions.To study this case, we varied the outdoor air temperature and we kept the lighting level on the floor constant. Fig. 5 gives the lighting levels measured on the floor of our room. The mean value is about 62.5W/m².
We give in Table 3 the main characteristics of the experiments we realized . The Rayleigh numbers are between 7.10^9 and $1.5.10^{10}$.

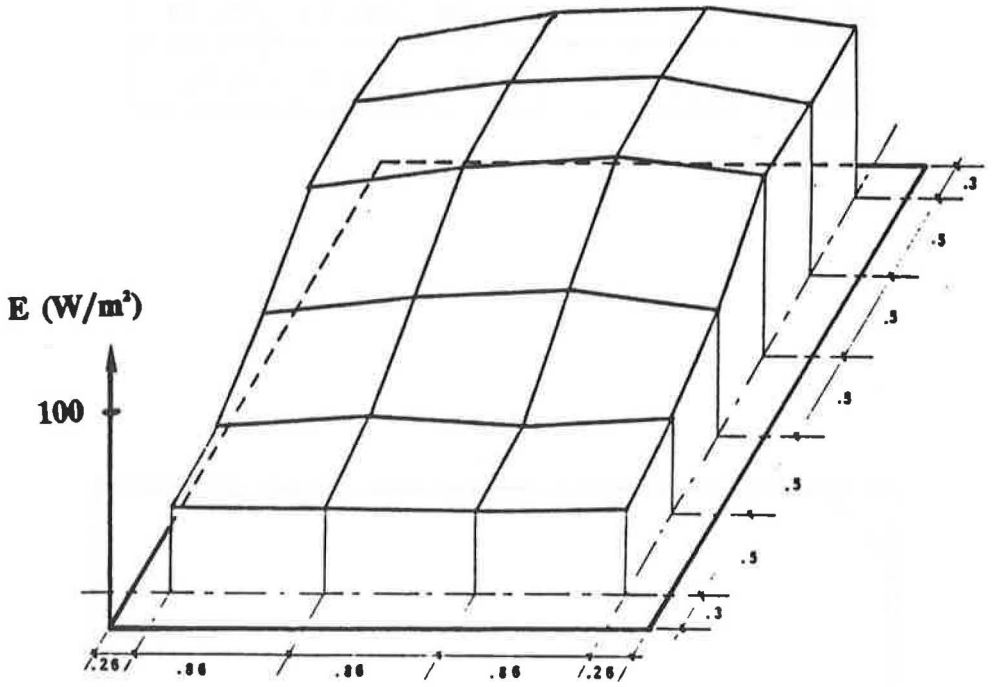

Fig. 5 . Lighting levels measured on the floor of the room.

Thermal Stratification Inside the Cavity. Figure 6 presents a typical result obtained during these experiments corresponding to a 0°C outdoor air temperature. This global behavior can be described in a first approach by a large isothermal core connected to a cold vertical boundary layer flow along the facade and to a more disturbed region with higher gradients along the floor.
All the facts pointed out by the rough analysis of the thermal field are confirmed by the study of the vertical thermal profiles inside the room. Fig. 7 represent the evolution of these thermal profiles with the decrease of the outdoor temperature which corresponds to a decrease in the Rayleigh number. The large central core of the cavity is not affected at all by a change in Rayleigh number, and it remains isothermal. We can notice also that a decrease in Rayleigh number leads to a smaller gradient close to the floor and a less perturbated thermal profile.The dimensionless central temperature varies from 0.2 to 0.3 in this set of experiments.

Table 3. Main Characteristics of the Experiments Realized with a Heated Floor.

EXPERIM.	HF.1	HF.2	HF.3	HF.4
T_o (°C)	40.66	38.45	35.55	33.40
ΔT (°C)	5.66	7.69	9.25	11.20
$Ra.10^{-8}$	6.8	9.5	12.0	15.0
T_c (°C)	41.79	40.58	38.33	36.92
T_c^*	0.20	0.28	0.30	0.31

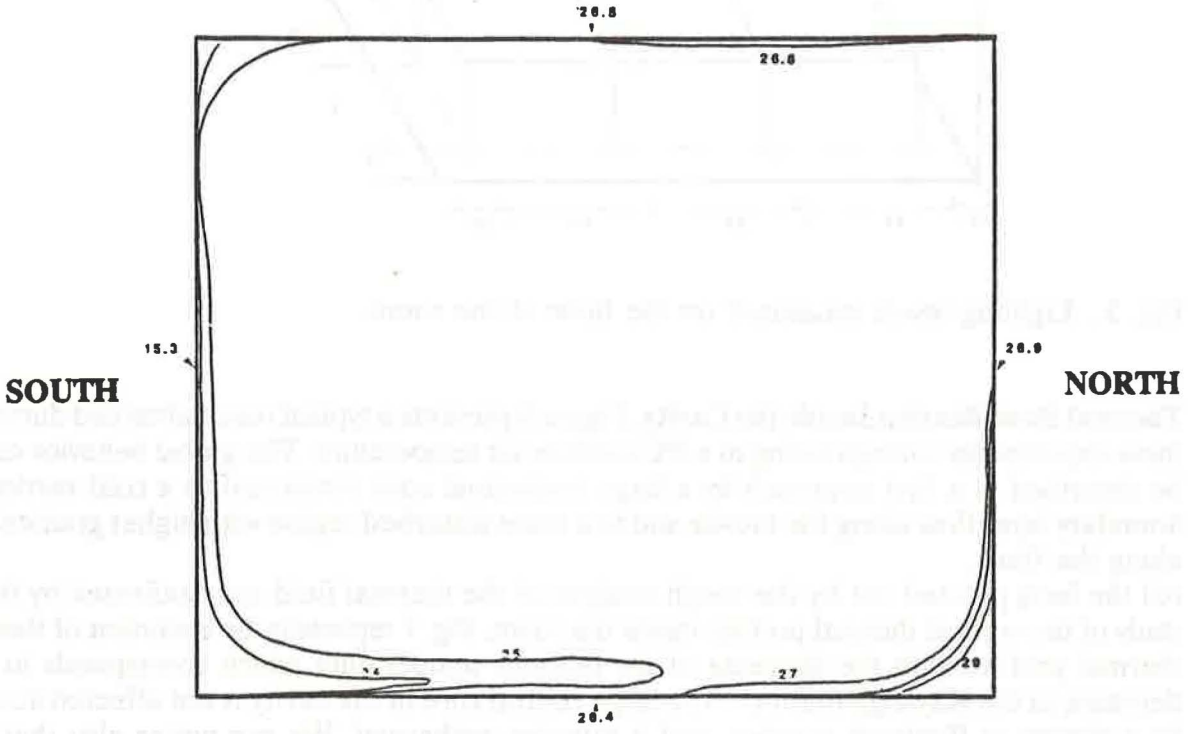

Fig. 6. Isothermal Lines in the Vertical Midplane of the Cavity.
(Heated Floor)

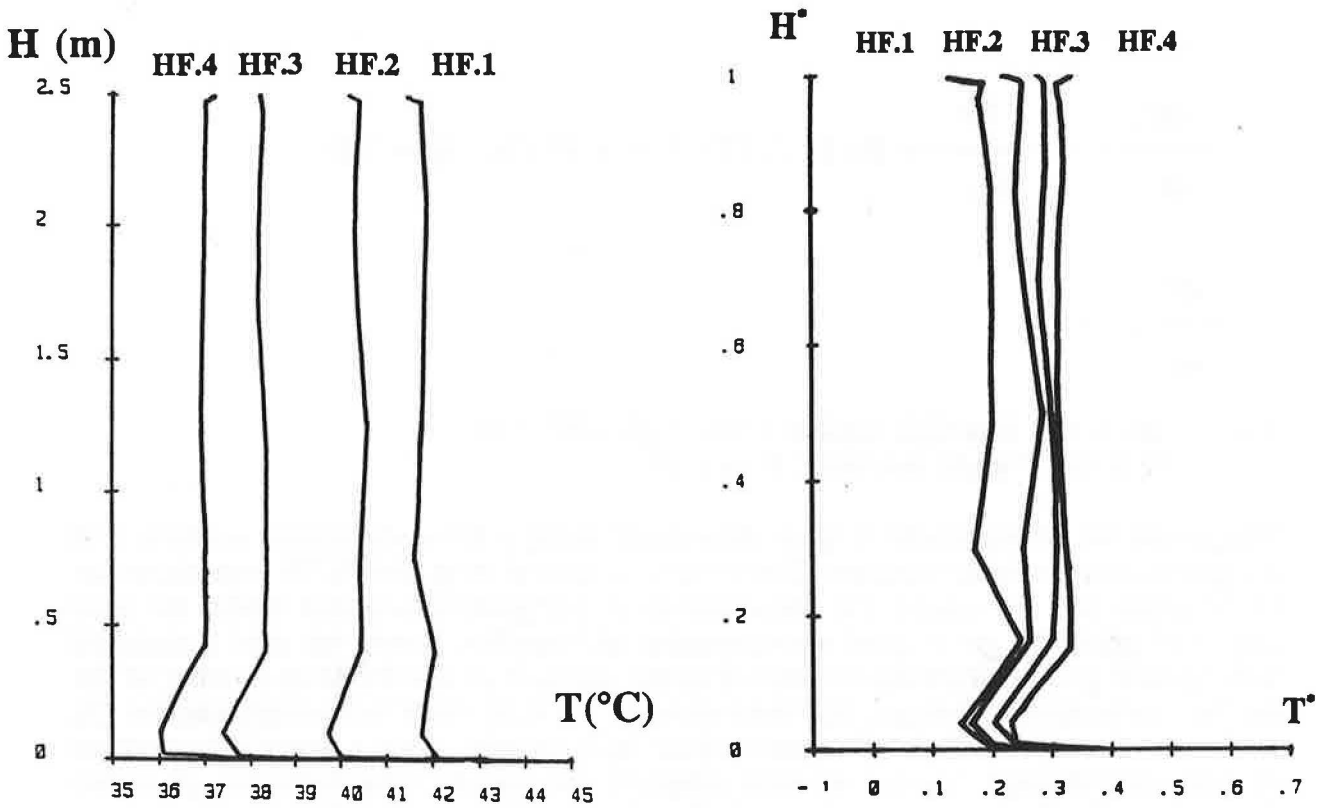

a) Real Temperature (b) Dimensionless Temperature

Fig 7. Influence of Outdoor Air Temperature on Vertical Temperature Profiles at the Center of the Cavity. (Heated Floor)

Numerical approaches

Laminar Flow

The experiments presented in the first section are absolutely necessary to well understand natural convection in cavities with heated horizontal surfaces. However, these full scale experiments are hard to realize and necesarily limited by the number and location of the sensors, the boundary conditions, and the ability to predict a reasonable interpolation between the points of measurements. This is one of the reasons why we have developed numerical simulations of natural convection flows in cavities in parallel with the experimental work.

At first we limited our investigation to laminar flows in bidimensionnal cavities (3).

The governing equations are the Navier Stokes equations written in their Boussinesq Oberbeck approximation. The reference length is the height of the room, the reference time is obtained from the thermal diffusion inside the cavity ($t = H^2/a$), this gives also the scale of velocities ($v = a/H$). The reference temperature is the same as defined before. These scales lead to a general writing of the equations in dimensionless form.

$$\text{div } V = 0$$

$$\frac{dV_i}{dt} = -\frac{\partial P}{\partial x_i} + Ra\ Pr\ \delta_{i2}\ (T - 0.5) + Pr\ \Delta V_i \quad (i = 1,3)$$

$$\frac{dT}{dt} = \Delta T$$

where Ra is the Rayleigh number ($Ra = g\beta\Delta TH^3 / \upsilon a$)
Pr is the Prandtl number ($Pr = \upsilon / a$)

The whole set of equations is then discretized using a finite difference scheme, and integrated over controle volumes. The pressure is solved using SIMPLER procedure due to Patankar (4). To ensure the conservation of all quantities in our model we used staggered grids. To get a good representation of boundary layers, we used a standard Tchebycheff grid in which the number of nodes depends on the Rayleigh number of the problem to be solved. This code has been tested on De Vahl Davis' benchmark solution (5), and other references avalaible for laminar flows (6,7). In order to get a better interpretation of our experimental results, we first simulate the steady state behavior of a two dimensionnal cell representing the vertical mid plane of our cavity. For this purpose we used the dimensionless temperature profiles obtained experimentally along the surfaces of our cavity as input in our numerical simulations.

Heated Ceiling. Figure 8 represents the isotherms, streamlines and heat flux lines obtained in this configuration for a Rayleigh number of 10^7, which corresponds to a limit of existence of laminar flows. As we saw in the experiments, we observe just beneath the ceiling a strongly stratified hot zone. Furthermore the flow patterns show very low velocities in this region. The high velocity regions are located along the cold vertical wall, and by continuity, along the floor. Then the central part of the cavity only has a slow movement. In this configuration, heat transfers are dominated by transport phenomena, nevertheless, in the upper part of the cavity velocities are very small and heat transfer between the hot stratified zone and the rest of the cavity is weak. As shown by the strong thermal stratification of this zone, thermal diffusion is certainly the leading heat transfer process in this part of the room.

Heated Floor. The results obtained with a heated floor are given on Figure 9 for a Rayleigh number of 10^7.
In the experiments this configuration was characterized by a large isothermal core, but we had no information about the dynamic behavior of the cavity. With numerical simulations, even at lower Rayleigh numbers, the interpretation becomes easier.
First of all this configuration appears to be a very stable one without any particular convergence problem. Furthermore we can see that the upper part of the cavity is occupied by warm air which leads to the stability to this configuration.

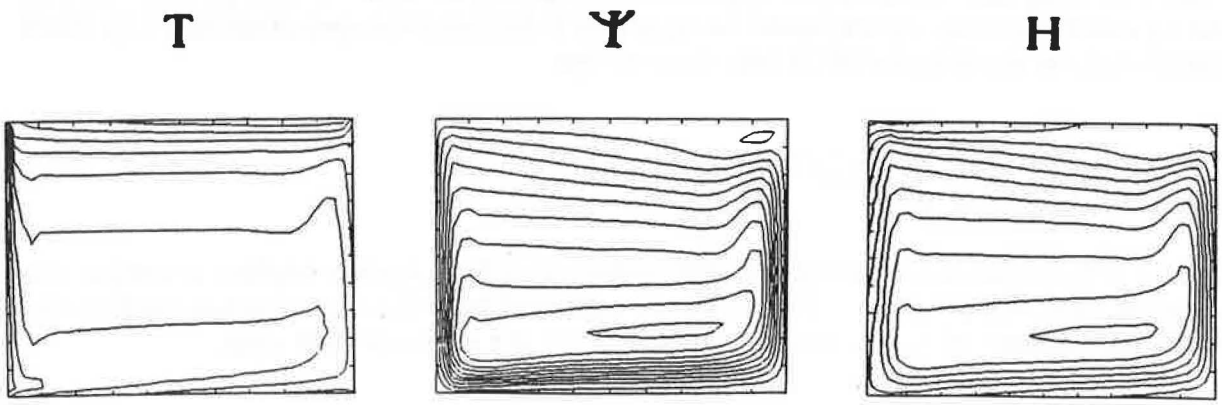

Fig. 8. Isotherms, Streamlines and Heat Flux Lines (Heated Ceiling Ra = 10^7).

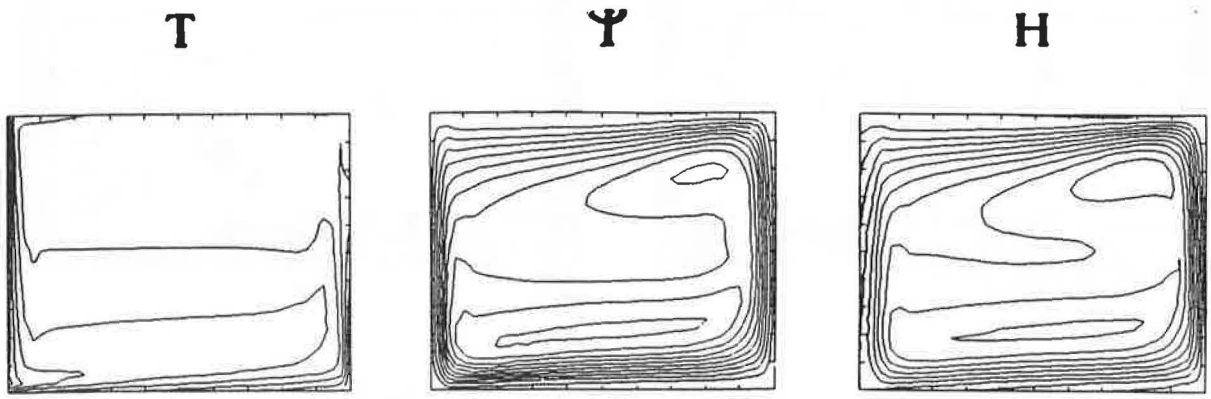

Fig. 9. Isotherms, Streamlines and Heat Flux Lines (Heated Floor Ra = 10^7).

The higher velocities are located along the cold facade and along the floor, the rest of the cavity sees a slow recirculating flow alimenting the boundary layer. The main heat transfer are due to transport between the cold facade and the ceiling, the other walls being quite adiabatic.

Unstationary Regimes.

In order to study the instationnary regimes developping at higher Rayleigh numbers, we used an other numerical code based on Spectral Tchebycheff approximation (7,8). Each quantity can be approximated in our domain by:

$$U(x,y,t) = \sum_{i=0}^{I} \sum_{j=0}^{J} u_{ij}(t)\, T_i(x)\, T_j(y)$$

Where $T_i(x)$ represents a Tchebycheff polynomial of order i. A semi-implicit discretization is used for time. We present on Figure 10 the results obtained in case of a heated floor for a Rayleigh number of 6.10^8, i.e; one decade from the experimental case.

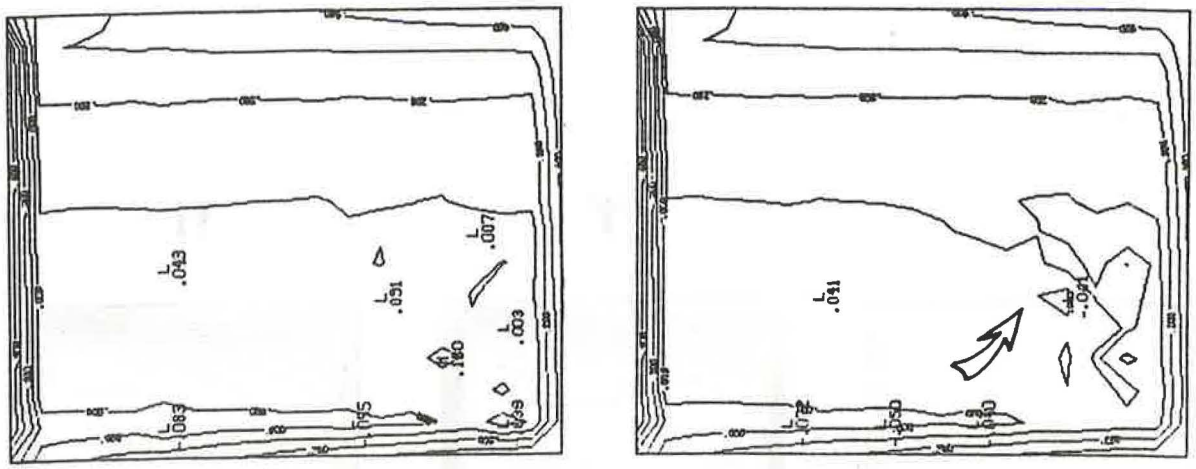

$t = t_0$ $\qquad$ $t = t_0 + 20s$

Fig. 10. Isotherms obtained at $Ra = 6.10^8$

In a general way, the flow becomes unstationnary after a Rayleigh number greater than 10^7. Then we obtain a periodic flow due to an unstability developping in the hot corner of the floor. This unstability is not strong enough to perturb the warm air located in the upper part of the cavity, and the result is a fluctuating behavior of the air in the right corner of the floor.

Turbulent Simulations.

Even using a sophisticated method, it is impossible to simulate by a direct approach the behavior of a room at high Rayleigh numbers, the time and space scales becomes too rich, and it is no more possible to have at the same time a good representation of the large structures of the flow, and a precise simulation of the small fluctuating eddies. The usual way is then to introduce a model representing the energy dissipation in the small structures and to look only at the general structures of the flow. The more common model is the so called k-ϵ model. The basic hypothesis of this model proposed by Boussinesq in 1877 is to represent the energy dissipation in the small structures of the flow by a turbulent viscosity which will be added to that of the fluid itself. This turbulent viscosity is then related to the turbulent kinetic energy k and its rate of dissipation ϵ.
Hence, we obtain a new set of transport-diffusion equations which are solved by using the same method used in the laminar case (9). In our turbulent model all the boundary conditions are defined at the very limit of the domain in order to avoid the use of wall functions. This solution requires of course a very precise description of the boundary layer, and we use a thiner grid with various nodes inside the laminar sublayer itself.

Heated ceiling. We present on Figure 11, isothermal lines and streamlines obtained in simulating one of our experiments. The results obtained show a good agreement with experimental results. We found the strongly stratified zone just beneath the ceiling, and the stratification in the center of the cavity is coherent with the experiments. This result confirms that in the upper part of the room the heat transfer by convection is weak. Heat transfer in this region is dominated by diffusion.

Heated Floor. As for the preceding case, we show in Figure 12 the results obtained when simulating the behavior of the mid plane of floor-heated-room. The agreement with experimental data shown in Figure 6 is good. The cold air coming down from the cold boundary layer is heated by the floor as a forced convection flow, transported upward by the main flow along the warm vertical wall, and then entrained by a slow movement through the cavity.

Conclusion

The experience we got from a complementary analysis coupling real scale experiments in controlled environment and numerical simulation of natural convection at high Rayleigh numbers is fundamental for the understanding of the thermal couplings in a heated cavity.
If experiments are absolutely necesary, they are not able to deliver all the information they contain, the number of sensors, their characteristics and their location are intrinsec limitations of an experiment.

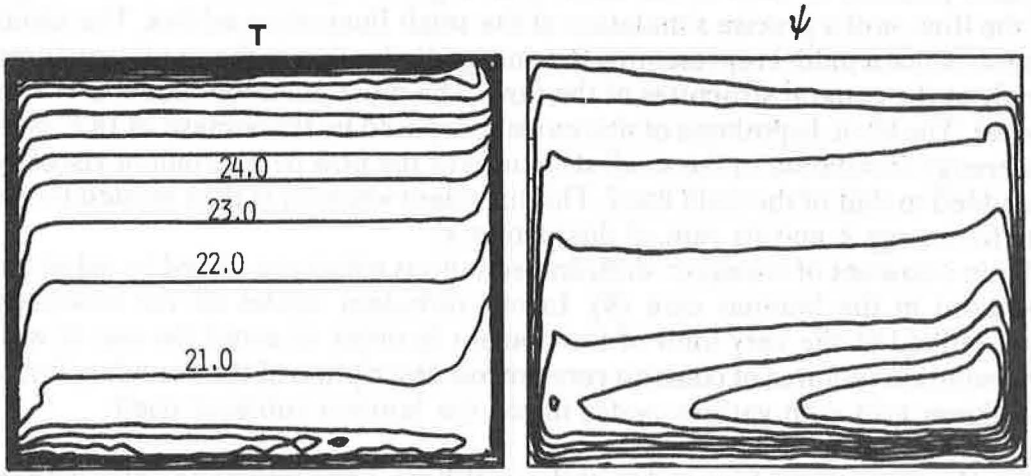

Fig. 11. Isotherms and streamlines (Heated Ceiling Ra= 10^{10})

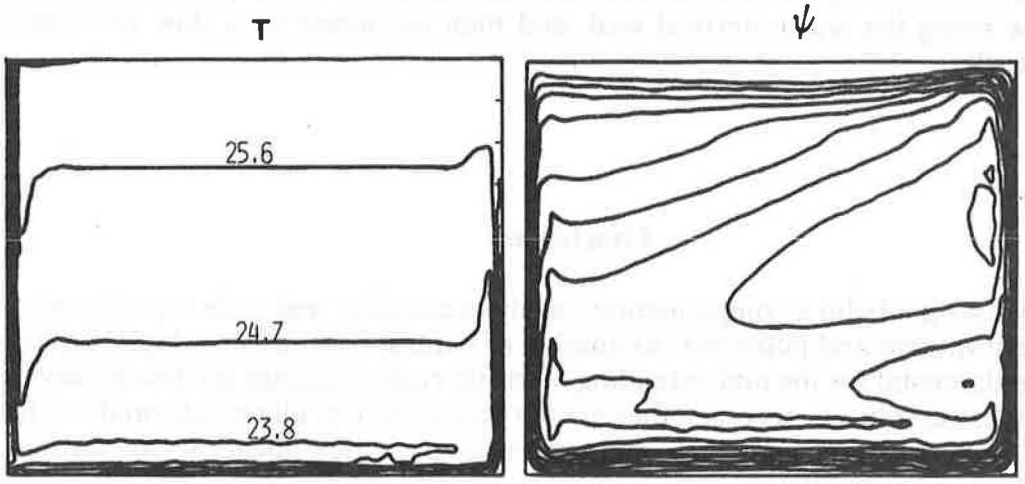

Fig. 12. Isotherms and streamlines (Heated Floor, Ra= 10^{10})

On the other hand, we are not able to develop today a general numerical code predicting the coupled heat transfers in such a cavity. Nevertheless, using both experimental and numerical analysis, we are now able to characterize and explain most of natural or mixed convection flow we find in building physics. The perspectives of such work should be now to develop and validate simplified approaches or zonal models able to predict the global behavior of a room and not too heavy to permit their introduction in more general codes simulating thermal behavior of buildings.

Aknowledgements. This work has been supported by CNRS/PIRSEM " National Scientific Research Center" and AFME " French Agency for Energy Management" within the frame of a National Research Programm on Natural Convection in Buildings, the numerical calculations have been performed on the Cray 2 of CCVR " Vectorial Computer Center for Research Applications".

References.

(1) Allard F. Contribution à l'étude des transferts de chaleur dans les cavités thermiquement entrainées à grand nombre de Rayleigh. Thèse de Doctorat ès Sciences, INSA de Lyon, 1987.

(2) Allard F., Brau J., Inard C., Pallier J.M. Thermal experiments of full-scale dwelling cells in artificial climatic conditions. Energy and Buildings, 10 (1987) pp 49-58.

(3) Simoneau J.P., Inard C., Allard F. Numerical approach of interaction between an injection and laminar natural convection in a thermally driven cavity. ASME Winter Annual Meeting, Chicago, 1988, Vol 99, pp 45-51.

(4) Patankar S. V. Numerical heat transfer and fluid flow. Mac Graw Hill Edit. London 1980.

(5) De Vahl Davis G. Natural convection in a square cavity. A Benchmark numerical solution. International Journal for Numerical Methods in Fluids, 1983, Vol. 3, pp 249-264.

(6) Le Quéré P. Humphrey J.A.C Description of calculation Scheme for thermally driven cavity Flow. Numerical solutions for a comparison problem on natural convection in an enclosed cavity. Computer science and system division AERE Harwell 1981, pp 97-102.

(7) Haldenwang P. Résolution tridimensionnelle des équations de Navier Stokes par méthodes spectrales Tchebycheff. Thèse de Doctorat ès Sciences, Université de Provence, 1984.

(8) Haldenwang P., Allard F., Labrosse G. Approche numérique de la convection naturelle à haut nombre de Rayleigh. Société Française des Thermiciens, Paris, May 1986.

(9) Simoneau J. P. Etude de l'interaction entre un jet et la convection naturelle dans une cellule d'habitation. Ph D Thesis, INSA de Lyon, 1989.